Polycyclic aromatic hydrocarbon record in an urban secondary carbonate deposit over the last three centuries (Paris, France)

Julia Garagnon, Yves Perrette, Emmanuel Naffrechoux, Edwige Pons-Branchu

Polycyclic aromatic hydrocarbon record in an urban secondary carbonate deposit over the last three centuries (Paris, France)

Julia Garagnon, Yves Perrette, Emmanuel Naffrechoux, Edwige Pons-Branchu

PII: S0048-9697(23)06056-4

DOI: https://doi.org/10.1016/j.scitotenv.2023.167429

Reference: STOTEN 167429

To appear in: *Science of the Total Environment*

Received date: 27 July 2023

Revised date: 20 September 2023

Accepted date: 26 September 2023

Please cite this article as: J. Garagnon, Y. Perrette, E. Naffrechoux, et al., Polycyclic aromatic hydrocarbon record in an urban secondary carbonate deposit over the last three centuries (Paris, France), *Science of the Total Environment* (2023), https://doi.org/10.1016/j.scitotenv.2023.167429

Polycyclic Aromatic Hydrocarbon record in an urban secondary carbonate deposit over the last three centuries (Paris, France)

Julia Garagnon [a,b,*], Yves Perrette [b], Emmanuel Naffrechoux [b], Edwige Pons-Branchu [a]

[a] LSCE/IPSL, UMR 8212CEA-CNRS-UVSQ, Université Paris-Saclay, Orme des Merisiers F-91191 Gif-sur-Yvette, France

[b] EDYTEM (CNRS/USMB/MCC), Bâtiment Pole Montagne, Campus Scientifique, 73376 Le Bourget du Lac Cedex, France

[*] corresponding author, *E-mail address*: julia.garagnon@lsce.ipsl.fr

---

K E Y W O R D S

- Speleothems
- Organic matter
- PAH
- Organic geochemistry
- Urbanization
- Anthropization

A B S T R A C T

Preserving water resources and limiting pollution are central environmental issues in the current context of intense anthropization. Among organic pollutants, polycyclic aromatic hydrocarbons (PAHs) are commonly analysed as part of water quality assessments. After being emitted into the atmosphere, these persistent organic pollutants are deposited on the continental surface, where they are transported to the aquatic environment by run-off and infiltration waters. Mainly due to anthropogenic emissions, PAHs can therefore be considered as a proxy for human activities. Urban secondary carbonate deposits (USCDs), similar to cave speleothems, have recently been studied for their potential as natural archives of water quality. However, USCDs have never been used to trace water organic pollution and only a few studies on PAHs in speleothems are available. This study focuses on a well dated USCD covering the last 300 years from the Great Aqueduct of Belleville (north-east of Paris, France). The aim is to determine the nature and variation of trapped organic compounds over time and to discuss their origin, transport, and link with changes in soil occupation due to human activities. To do so, high-resolution solid-phase UV fluorescence imaging analyses were combined with chemical analyses of PAHs and organic carbon carried out on low-weight samples. The results show that PAHs have been present in urban surface water for 300 years. Over the last few decades, a 7-fold increase is observed, accompanied by a change in the pollution source, enriched in high-molecular-weight PAHs, probably linked to urban dust. This study also reveals modes of transport directly influenced by changes in the soil occupation that are very different from those usually encountered in natural environments. This work thus paves the way for a better long-term understanding of the impact of human activity on the transfer of pollutants to sub-surface waters.

1. Introduction

Over the last hundred years, the use of freshwater in the world has increased by six and is expected to be 20% to 30% higher than the current level in 2050 (Burek et al., 2016) at a time when 3.9 billion human beings will suffer from difficult access to water due to global warming (Ligtvoet et al., 2014). Preserving water resources is therefore a key environmental issue in the current context of intense human activity. Both the IPCC and the United Nations have underlined the urgent need to increase the means devoted to managing and protecting this resource (Bates et al., 2008; Jiménez Cisneros et al., 2014; United Nations and Department of Economic and Social Affairs, 2022). The use of non-conventional water sources such as rainwater, spring water or sub-surface groundwater could be one of the solutions to the water shortage in densely populated areas. However, one of the main issues concerning this resource is the qualitative dynamics of this water, linked to the impact of human activities on the surface.

Polycyclic aromatic hydrocarbons (PAHs) are commonly quantified in water quality analysis because of their carcinogenic properties for humans (Baek et al., 1991). These semi-volatile organic compounds (SVOC) are mainly due to anthropogenic emissions (Du and Jing, 2018). Fossil fuel combustion (transport, residential heating...), waste incineration, coal gasification, petroleum cracking and the production of coke, tar pitch and asphalt have been identified as important anthropogenic sources of PAHs (Hangebrauck et al., 1967; McVeety and Hites, 1988). More generally, there are two main sources of PAHs in the urban environment: (i) pyrolytic PAHs formed by the incomplete combustion of organic matter (wood, fossil fuels), and (ii) petroleum PAHs from spilled oils and petroleum products (Brown and Peake, 2006; Ngabe, 2000; Takada et al., 1991). The former are emitted into the atmosphere while the latter are more generally introduced directly into the soil. Deposition processes represent important mechanisms of PAH removal from the atmosphere to the Earth's surface. Once deposited on the continental surface, runoff is an important pathway of PAHs to the aquatic environment (Müller et al., 2020). Their study in natural archives such as marine or lake sediments has enabled their origin and/or their evolution through time to be discussed in certain cases for well dated sequences (Arias et al., 2010;

Guo et al., 2007; Pereira et al., 1999) but few studies have been carried out on PAHs in speleothems (Argiriadis et al., 2019; Perrette et al., 2008) due to their low concentrations and the analytical difficulties involved in extracting them. Considered as sensitive recorders of past changes, speleothems offer an underinvestigated natural archive for the reconstruction of water quality. In artificial urban structures such as aqueducts or tunnels, urban secondary carbonate deposits (USCDs) similar to speleothems from caves were recently studied for their potential as natural archives for past sub-surface water quality evolution through time (Pons-Branchu et al., 2014). However, USCDs have never been used to reconstruct water pollution by organics over time.

This study focuses on a well-dated USCD covering the last 300 years, fed by urban groundwater in the Belleville Great Aqueduct beneath the city of Paris city (France). Previous studies of USCDs from this aqueduct have shown that time variations of heavy metals, rare Earth elements (REE) and sulphur, due to different sources and causes of variation, are linked with urbanisation, and more generally soil occupation changes (Pons-Branchu et al., 2017, 2015, 2014). The present work traces the quantitative evolution of organic content trapped in a USCD over the last few centuries, focusing on PAH pollution and the link with organic matter (OM) to which PAHs are generally bound (Santschi et al., 1997). Their transport by water, as solutes or adsorbed on particles, remains a key point in order to be able to reconstruct water quality in urban areas. Indeed, during their transport, PAHs can undergo fractionation between water and soil linked to their physico-chemical properties (aqueous solubility (S*) and octanol-water partition coefficient (Kow). PAHs considered to have a low molecular weight (LMW) are generally more soluble in water and bind less to OM (low Kow), whereas PAHs with a heavy molecular weight are less soluble in water and complex more with OM (high Kow). The first aim of this study was to determine the nature and variation in PAHs and organic matter (OM) trapped in a well-dated USCD, through the development of a robust analytical protocol for the determination of small quantities of PAHs in relatively small quantities of USCD and the use of UV fluorescent measurements. The second aim of this study was to understand their origin and transport in relation to changes in land use due to human activities, by cross-referencing the PAH data with the content of OM and inorganic trace elements.

2. Material and methods

2.1. Site and samples

The Great Aqueduct of Belleville (BEL) is a 1050m long underground gallery in the north-eastern part of Paris (France). It is part of a larger historical network, known as "Northern Springs", that drains waters from two independent groundwater levels, one within the well-sorted Fontainebleau sands and the other one within Brie limestone (Fig.1). This network was used to supply drinking water to public fountains between the 12th and 19th century (Clément and Thomas, 2016). Still supplied with water from several drains, these waters are no longer used and end within the rainwater harvesting system. The calcareous water has favoured the deposition of USCDs in some parts of the aqueduct.

BEL2 sample is a 45 mm thick and finely laminated USCD that was sampled in the middle part of the Great Aqueduct. The gallery, oriented N/S, lies about 5-10 m below Levert street level near its intersection with Pyrénées street. BEL2 developed on the wall of the gallery and receives groundwater and surface water seeping directly from the roof of the gallery. The water infiltration time in the catchment area has been estimated at 3-4 months (R. Branchu (Cerema), pers. com, n.d.). Today, the water infiltrating from the roof of the gallery certainly passes through a layer of fill enriched in gypsum between 1 and 5 m thick which overlies the Brie limestone (Fernandez, 2018; Pons-Branchu et al., 2017). A robust chronology of BEL2, based on the cross-referencing of absolute and relative dating techniques (U/Th and lamina counting) carried out by Pons-Branchu et al. (2014), determined that 300 years of records ± 15 years (between 1711 and 2011 CE) are contained in these deposits exhibiting a constant growth rate.

In BEL2, 18 levels were sampled within the growth axis for PAH and Organic Carbon (OC) analysis. Sampling was performed using a wire saw equipped with a 0.6 mm diamond wire to minimize the waste

calcite (BEAPV saw/ Escil Wire). The USCD was first sliced and then cut to obtain blocks of about 1 g, incorporating around 15 years of recordings. Three blocks following the lamination were used (3 g) for each sample. The samples were wrapped in aluminium foil and kept in sealed bags. Based on Hartland et al. (2014), about 90 mg of calcite powder were estimated as necessary for liquid fluorescence and OC analysis. Sampling was done using a micromill equipped with a 1 mm diameter drill bit. The sample was drilled to a depth of 3.5 mm and then horizontally to a width of 10 mm with a 1 mm pitch following the lamination. The resulting powder was collected and wrapped in aluminium foil. According to the sampling depth, an age was estimated for each sample using the chronology previously developed on this USCD (Pons-Branchu et al., 2014) (S2).

2.2. Analytical

2.2.1. PAH extraction and quantification

The procedure for PAH extraction and quantification was established on the basis of the work of Argiriadis et al. (2019) and Perrette et al. (2008). Briefly, calcite is acid-dissolved and PAHs are extracted with dichloromethane, then analysed by HPLC-fluorometry.

To prevent contamination, the tools and glassware were washed in two stages: a 2-hour hot detergent bath, then after rinsing with tap water, a 2-hour nitric acid bath, and finally a rinse in an osmosed water bath.

Each calcite fragment was first weighed using a microanalytical balance and then sonicated three times with dichloromethane to decontaminate the outer surface from PAHs adsorbed (Wynn and Brocks, 2014).

2.2.1.1. PAH extraction

The calcite fragment was transferred to sealed, clean 60 mL vial with a pierceable cap and spiked with 15 ng of acenaphthene D10, anthracene D10, and benzo[a]anthracene D12 (AccuStandard Certified Reference Materials), as internal standards before addition of 15 mL of dichloromethane (Honeywell, Chromasolv for HPLC) and 5 mL of UHQ water. Acid digestion was carried out with 10 mL of HCl (Carlo Elba, 34-37% RS Superpure for trace analysis), added via a glass syringe through the septum. Each vial was shaken by hand until the calcite was completely dissolved.

The obtain acid water/dichloromethane emulsion was then extracted three times with 5 mL of dichloromethane. After organic phase separation, Na_2SO_4 powder was added to the 30 mL of dichloromethane in order to eliminate the residual water. The organic extract was evaporated at 40°C under nitrogen stream in a Turbovap (TurboVap II, Caliper Life Sciences), and then filtered to 0.22 µm and transferred to an 8 mL vial. After addition of 100 µL of dimethylsulfoxide (Thermo Scientific, LC-MS Grade), evaporation under reduced pressure of nitrogen was gently continued to a final volume of 100 µL. The solution was then taken up with 100 µL of methanol (Honeywell, Chromasolv for HPLC) to obtain a final volume of 200 µL.

2.2.1.2. PAH quantification

PAH analyses were carried out according to the method published by (Perrette et al., 2013) with a Perkin Elmer HPLC device (serie 200) coupled with a fluorometric detector (PE serie 200a). The separation was performed using a Macherey Nagel C18 column (EC 4/3 nucleosil 100-5 C18 PAHs) and pre-column (EC 250/4.6 nucleosil 100-5 C18 PAHs) placed in an oven set at 40°C. PAH elution was performed with a gradient from 80:20 methanol/water mixture to 100% methanol over a 22 min period at a flow rate of 1 $mL.min^{-1}$. The 100% methanol level was maintained for a further 19 min at 1 $mL.min^{-1}$ and 15 min at 1.6 $mL.min^{-1}$, ending with 3 min at 80:20 methanol/water at 1 $mL.min^{-1}$ flow rate. Fluorescence detection was programmed with 9 excitation (from 225 to 300 nm) and emission (between 320 and 500 nm) wavelength pairs adapted to the sensitivity of each of the 15 PAH (naphthalene (N), acenaphthene (ACE), fluorene

(FLU), phenanthrene (PHE), anthracene (ANT), fluoranthene (FLA), pyrene (PYR), benzo[a]anthracene (BaA), chrysene (CHR), benzo[b]fluoranthene (BbF), benzo[k]fluoranthene (BkF), benzo[a]pyrene (BaP), benzo[ghi]perylene (BghiP), dibenzo[a,h]anthracene (DbahA), and indeno[1,2,3-cd]pyrene (IP)). Fluorescence data were processed using the HPLC Manager D-6000 v.5 software. The quantification was calibrated by an external method using 6 standard mixtures of 16 PAH reference materials (EPA 610). Detection limits (LOD) and quantification limits (LOQ) were calculated using the calibration lines method with three and six times the standard deviation respectively. LOD were in the range 0.02 – 0.44 $ng.g^{-1}$, and LOQ between 0.03 and 0.76 $ng.g^{-1}$ depending on the PAH congener. Procedural blanks were analysed with the samples to check for possible contamination. Concentrations measured below blank (LOB) or LOD were assumed to be zero. Uncertainties were determined from spiked deuterated PAHs measured for each sample. A 95% confidence interval (IC(95)) was calculated and applied according to the log KOC and log KOW of each PAH measured; IC(95) was 42% if log KOC or KOW < 5 otherwise IC(95) was 27%.

2.2.1.3. Procedure control

To evaluate the accuracy of the procedure, each sample and blank were spiked with a mixture of three deuterated PAHs (acenaphthene D10, anthracene D10, benzo[a]anthracene D12). The yield of spiked deuterated PAH measurements was estimated to be 70% on average so concentrations were not corrected from the yield. Procedural blanks were analyzed, and all measured values were found to be below LOD except for naphthalene (0.6 $ng.g^{-1}$) and phenanthrene (0.05 $ng.g^{-1}$). As replicating from the same sample was not possible, control points were carried out on samples cut from another slice of BEL2 but following the same sampling areas. One of the control points, BEL2_7R, was identified as an outlier and was therefore not considered. Control point measurements show a difference of 32% on average with the initial PAH concentrations measured. This variability is certainly due to the lateral variation in the stratigraphy of BEL2 sample. The trend between the two series of points is similar (r_s= 0.82).

2.2.1.4. Data analysis

The concentration of each compound is given in Table 1 and has been represented (Fig.2) as PAH profiles with the relative proportion of each PAH to the total of the 15 PAH to facilitate comparisons between the different periods. The percentage of low molecular weight (LMW) PAHs corresponding to PAHs with two or three rings (from ACE to ANT) and high molecular weight (HMW) PAHs with 4 to 6 rings (from FLA to IP) was also calculated.

2.2.2. Organic carbon and nitrogen analysis

For each sample, approximately 80 mg of powdered calcite was diluted with a small amount of water in a 40 mL vial and then dissolved with 12 N HCl. Water and HCl volume were calculated for each sample to obtain 1 mL solution at neutral pH. After complete dissolution, the solution was diluted with UHQ water to a final volume of 30 mL The solution was then sparged with N_2 for 5 minutes to strip CO_2 and reduce analysis time. Triplicates were realised from 200 mg of powder taken from the base of BEL2, homogenized, then split into 3 equal masses. After preparation, all samples were stored in a freezer and then thawed 24 hours before analysis. UHQ water and hydrochloric acid (Carlo Elba, 34-37% RS Superpure for trace analysis) were used for organic carbon (OC) and organic nitrogen (N) analyses. Tools and glassware underwent the same decontamination protocol as for PAHs. In addition, the glassware was muffled at 525°C for 2h.

OC and N analyses were carried out on a Shimadzu TOC-V_{CSN}. The analyzer was calibrated in Total Carbon (TC) mode from the Chemlab 100ppm standard and Total Nitrogen (TN) mode from Shimadzu KNO_3 powder. Series of standards (Chemlab, Sigma and homemade standards from potassium hydrogen phthalate $C_8H_5KO_4$ for TC and standard from Shimadzu KNO_3 powder for TN) and UHQ water blanks were run to check the calibration at the beginning, middle and end of the analysis.

The syringe was rinsed twice with the sample before analysis. The OC and TN analyses were performed simultaneously with a calibration range of [0-20] $mg.L^{-1}$ and [0-5] $mg.L^{-1}$ respectively.

The number of injections was set at two, and the maximum number of injections at three with an injection volume of 80 µL. Uncertainties were determined from triplicate results. A 95% confidence interval was calculated for TN and OC and applied to all samples.

2.2.3. UV Fluorescence measurements

2.2.3.1. Solid Phase Fluorescence (SPF)

SPF measurements were conducted using a fully modular spectrofluorometer as used in Moya et al. (2023). It consists of two Nd:YAG lasers emitting at 266 nm and 355 nm respectively. The spot size after focusing the laser on the sample was around 15 µm. Because the work was conducted on solid samples, the reflectance of the NIR diode used in the Nd:YAG laser was detected.

Laser Induced Fluorescence (LIF) in a steady state and NIR reflectance (NIRR) emissions were measured using a back-illuminated and thermoelectric-cooled CCD detector (Jobin-Yvon Sincerity) via a monochromator (Jobin Yvon MicroHr) equipped with an adjustable slit and a 300 g/mm diffraction grating centred at 600 nm giving approximately a 1 nm/px spectral resolution.

SPF measurements were performed along BEL2 sample in two dimensions to obtain continuous lines along the X axis and images with a 50 µm x 50 µm resolution. The images were obtained by stacking lines along the Y axis.

2.2.3.2. Data processing

All the fluorescence data were processed in Matlab using a supervised approach based on a least-squares method constrained by ranges for the position and size parameters. Each fluorescence spectrum was simulated by a linear combination of lognormal functions (Moya et al., 2023) with defined centers, widths, and surface (fluorescence intensity).

The fluorescence of chromophoric organic matter (COM) SPF spectra were simulated with 3 lognormal functions (λem. 340 nm ± 20 nm; 420 nm ± 20 nm; 500 nm ± 20 nm) at λex. 266 nm and only two at λex. 355 nm with an additional lognormal function for NIRR (812 nm ± 5 nm). To avoid the effects of crystallinity, a fluorescence intensity ratio was calculated from SPF data at λex. 266 nm between the fluorescence emission at 420 nm ($I_{\lambda\text{em.420 nm}}$) and 500 nm ($I_{\lambda\text{em.500 nm}}$) such that: $I_{\lambda\text{em.500 nm}} - I_{\lambda\text{em.420 nm}} / I_{\lambda\text{em.500 nm}} + I_{\lambda\text{em.420 nm}}$.

2.2.4. Statistical method

A Spearman correlation (expressed as r) was calculated in the previous section (2.2.1.3.) on the PAH procedure control to check that the variations between the samples and the control points were ordinal relationship. Bravais Pearson linear correlations were used for other data processing when linear relationship was assumed. Each R^2 and effective (n) are given. Robust statistical method was used to avoid outliers bias, as for BEL2_1. Supervised approaches were also used by selecting the data according with their scattering. This method enabled the isolation of groups with different behaviours.

3. Results

3.1. PAHs in BEL2

Total PAH concentrations (sum of the 15 PAHs) measured for the 18 samples ranged from 0.1 $ng.g^{-1}$ to 76.7 $ng.g^{-1}$ (see Table 1 and Fig.2). Except for the sample corresponding to the growth period after 1995 CE, the measured concentrations do not exceed 10.7 $ng.g^{-1}$ which seems relatively low compared to the concentrations measured by Perrette et al., 2008 but in line with the results from Argiriadis et al., 2019. Five increases in total PAH concentrations can be distinguished in Fig.2. A first increase in concentration is observed for the sample between 1747 and 1767 CE with a total PAH concentration of 10.7 $ng.g^{-1}$, a second one between 1830 and 1843 CE twice as low (5.7 $ng.g^{-1}$), a third one between 1884 and 1899 CE with concentrations similar to the first one (10.3 $ng.g^{-1}$), another one between 1929 and 1945 CE (6.4 $ng.g^{-1}$) and finally a last one, beginning in 1968 but increasing sharply between 1995 and 2011 CE, totaling 76.7 $ng.g^{-1}$ of PAHs, i.e. 7 times higher than the previous ones.

From the 1930s, the proportion of HMW PAHs has increased from about 13% or 0.9 $ng.g^{-1}$ to almost 97% or 74.1 $ng.g^{-1}$. Although the total concentrations are very low, the PAH profiles seem to change from 1803 CE with a clear increase in the proportion of benzo[b]fluoranthene and benzo[ghi]perylene, as well as the emergence of dibenzo[ah]anthracene, PAHs with very low solubility ($S^* << 1$ $mg.l^{-1}$). However, the 1960s marked a transition with the emergence of benzo[a]pyrene, followed by benzo[k]fluoranthene and indeno-pyrene.

In contrast, the increase between 1824 and 1899 CE is linked to an increase in proportion/concentration of naphthalene (50% /5.2 $ng.g^{-1}$). From the 1730s, naphthalene and acenaphthene, the most soluble PAHs in water (respectively $S^* = 32$ and 3.42 $mg.l^{-1}$), are found in significant proportions. The 1750s show an increase in these two PAHs. The PAH content of the USCD is characterized by the omnipresence of phenanthrene over time.

3.2.Organic content

3.2.1. Organic carbon and nitrogen content

The OC values measured are in the range of 1.6 to 3.2 $mg.g^{-1}$ (Table 2) which seems coherent with the values of OC already measured in speleothems from natural caves (Hartland et al., 2014; Quiers et al., 2015). TN values are very low, between 0.042 and 0.106 $mg.g^{-1}$. If point BEL2_9, corresponding to an organic carbon peak with a high value, is excluded, the coefficient of determination between TN and OC values, R^2 is 0.61.

3.2.2. UV fluorescence results

The SPF results focus on measurements carried out under λex. 266 nm. Although sometimes significantly present, the fluorescence emission at 350 nm (function 1 in Fig.3) remains clearly negligible compared to the λem. 420 nm and λem. 500 nm (functions 2 and 3 in Fig.3). The intensity ratio between fluorescence emissions at λem. 420 nm and λem. 500 nm is represented as a map on which the samples used for organic carbon and LPF analyses can also be identified in black (Fig.3). Here, the blue-shift corresponds to an increase in fluorescence emission around 420 nm, while the red-shift corresponds to an increase in fluorescence emission around 500 nm. The intensity ratio shows variations ranging between 0 and 1. The fluorescence intensity emitted around 500 nm dominated that emitted around 420 nm over all the spectra measured. The 1760s were characterized by a blue-shift, i.e. the transition from a period dominated by a marked fluorescence intensity at λem. 500 nm to a higher fluorescence intensity at λem. 420 nm. Then, from the 1850s onwards, a red-shift was observed until the end of the 19th century, when a rapid change to a blue-shift took place. A red-shift was also observed between the 1940s and 1980s.

4. Discussion

4.1. PAH sources

The concentrations measured in the sample are probably the result of a mixture of different sources as already shown by several studies in urban environments (e.g. Brown and Peake, 2006; Liu et al., 2010). In addition, PAHs can undergo alteration processes (e.g. biodegradation, photo-oxidation) and selective adsorption due to their different physico-chemical properties (Kow and aqueous solubility) from their source to the USCD. Once deposited on the continental surfaces, HMW PAHs are preferentially stored in the soils by adsorption on particulate OM, as the more soluble LMW PAHs can be easily transported in aqueous dissolved phase (Perrette et al., 2013).

For all these reasons, PAH molecular diagnostic ratio (MDR) values can vary from one environmental compartment to another and should be used with caution (Katsoyiannis et al., 2011; Katsoyiannis and Breivik, 2014; Tobiszewski and Namieśnik, 2012; Zhang et al., 2005). However, changes in some ratios over time, combined with historical information or source profiles, can provide important insights.

4.1.1. The ubiquity of phenanthrene since the 18th century

The PAH profiles in BEL2 are clearly dominated by phenanthrene (Fig.2), whose concentrations are relatively stable over time at around 1.5 $ng.g^{-1}$ on average. Relative concentrations range between 21 and 54 % of the total amount of PAHs, except for BEL2-1, which corresponds to the most recent period, where the relative concentration falls to 2%. This ubiquity of phenanthrene has already been reported in previous studies on PAHs. Desaules et al. (2008), in a large-scale study, showed that phenanthrene dominates all PAH profiles in the different types of Swiss soils. This observation was also highlighted by Grimalt et al. (2004) when they studied soils and lake sediments in the Tatras mountains of Poland. Phenanthrene is present in many PAH sources (Ravindra et al., 2008) which could explain its presence in many environmental compartments and different environmental media. A significant content of phenanthrene has been observed in agricultural fire emissions (Kakareka and Kukharchyk, 2003), in urban runoff (Gonzalez et al., 2000; Hoffman et al., 1984) and sewer particles (Rocher et al., 2004). In addition,

compared to its structural isomer, anthracene, phenanthrene is more thermodynamically stable (Soclo et al., 2000) and shows a high sorption onto humic acids (Staninska et al., 2015).

4.1.2. Recording of intensive urbanisation

Fluoranthene (FLA) and pyrene (PYR) are two isomers and are often associated in analyses of natural matrices (Soclo et al., 2000; Suman et al., 2016; Yu et al., 2014; Zhang et al., 2008). They are considered as typical pyrogenic products derived from the high-temperature condensation of lower molecular weight aromatic compounds (Soclo et al., 2000). In BEL2, as for phenanthrene, fluoranthene and pyrene have been present since 1711 CE. Relative concentrations of fluoranthene and pyrene ranged from 3 to 12 % and 4 to 13 % respectively. The FLA/(FLA+PYR) ratio is often used in MDR to discriminate between pyrogenic (> 0.4) and petrogenic (< 0.4) products as well as fuel type (De La Torre-Roche et al., 2009). Ideally, a corrective factor taking transport and time effects into account should be applied when calculating the ratio; however, none of the corrective factors present in the literature apply to speleothems in an urban environment (Zhang et al., 2005). A Monte Carlo method was used to compute the uncertainties in the FLA/(FLA+PYR) ratio. Random sampling of the analytical uncertainties of each parameter was performed using a Box-Muller transformation (Box and Muller, 1958) for each of the 10 000 iterations of the Monte Carlo procedure. Here, the ratio shows a sudden change in behaviour (Fig.4), shifting around the 1850s from a phase with values mostly above 0.5, except for a few samples with a very low ratio, to a stable phase with values between 0.4 and 0.5 except for one sample between 1945 and 1960 CE.

This shift occurred during the urbanisation phase and has continued to the present day (Fig.4). The urbanisation phase was triggered by a major increase in population in 1825 and resulted in significant modification of the overlying soil (Huard, 2019). Essentially agricultural land was then replaced on a massive scale by residential buildings until the end of the 19th century (Fig.4). In addition, this period also

corresponds to the Industrial Revolution, in which an agricultural society evolved into an urban and industrial society. The change in human activities probably led to a change in sources. The decrease in the FLA/(FLA +PYR) ratio therefore highlights a change that seems to have been caused by the massive urbanisation of Belleville and its surroundings. This change may be linked to a modification in source, in PAH transport, or both. If we consider the cut-off values for the FLA/(FLA+PYR) ratio to be valid, they appear to indicate a shift from a period dominated by pyrolytic emissions, mainly produced by the combustion of wood, coal or plants (> 0.5), to a period dominated by emissions that are still pyrolytic but essentially from fossil fuels (0.5 < > 0.4). However, even if these hypotheses seem consistent with history, they should be treated with caution, as surface modifications, such as soil sealing by buildings and the creation of fills, may have played an important role in modifying the conditions under which PAHs are subsequently mobilised and transported, thus changing the limits of this ratio.

Moreover, changes to the soil surface associated with urbanisation also appear to have impacted the OM content transported by infiltration water, as the solid-phase UV fluorescence ratio (Fig.3) used to observe variations in the quality of COM shows a change during the period of urbanisation between 1850 and 1900. This period is marked by a red-shift which corresponds to an input of higher-weight or more aromatic organic molecules.

4.1.3. Change of source in the 1950s

LWM PAHs in BEL2 correlate strongly with total PAHs from 1711 to 1960 CE (Fig.5.a, R^2=0.996, n=14). Between 1960 and 2011 CE (samples 3 to 1), an enrichment in HMW PAHs is observed (Fig.5.a). This change is also identified in the evolution of the proportions of LMW and HMW PAHs (Fig. 2), where a significant increase in the proportion of HMW PAHs is recorded. In addition, during this period, an emergence of the carcinogenic benzo[a]pyrene, benzo[k]fluoranthene and indeno-pyrene is observed in the PAH profiles (Fig.2). All these observations, combined with the absence of any major urban transformations at the surface at that time (Fig.4), suggest a change in the source of PAHs since 1960 CE.

Previous studies on gross bed solids from Parisian combined sewer deposits (Rocher et al., 2004), urban sediments impacted by stormwater runoff in the USA (Stout et al., 2004) or road debris and the suspended sediment component of urban runoff in New Zealand (Brown and Peake, 2006) also show a very high proportion of HMW PAHs, implying very low LMW/HMW ratios, which the authors link to a pyrogenic origin, indicating a predominance of pyrogenic sources in the final mixture. Benzo[ghi]perylene and indeno-pyrene are present in significant proportions (Fig.2 and 5.b.). They present a ratio between 0.2 and 0.5 implying a fossil fuel combustion source (Tobiszewski and Namieśnik, 2012), which is also confirmed by the FLA/(FLA+PYR) ratio (Fig.4).

As motor vehicle emissions are the major sources of emissions in urban areas (Freeman and Cattell, 1990; Shen et al., 2011; Tuominen et al., 1988), the rapid expansion of car production in France during this period (Méot, 2009) is thus certainly responsible for one of the main sources of pyrogenic emissions from fossil fuel combustion. The increase in road traffic contributes to the formation of street dust and urban dust, which deposit on soils. Asphalt also contains significant amounts of PAHs and a mixture of petrogenic and pyrogenic compounds (Brandt and De Groot, 2001; Brown and Peake, 2006). The asphalting of streets in Paris and the Belleville district gradually replaced cobblestones from the 1980s. This sealing of surfaces facilitates the mobilisation and transport of PAHs by road wash water and urban run-off (Brown and Peake, 2006). Urban dust, from a certified sample (SRM 1649a), presents a profile enriched in HMW PAHs similar to that measured in BEL2-1 (Fig.5.b). Urban dust seems to explain the presence of high relative concentrations in HMW PAHs in BEL2_1, particularly in benzo[a]anthracene, chrysene, benzo[a]pyrene, benzo[k]fluoranthene, benzo[ghi]perylene and indeno-pyrene (Fig.5.b, R^2=0.99, n=6). Other contaminants may also be present in street dust, such as metallic elements (Brown and Peake, 2006). This seems to be confirmed by an increase in Pb and REE signals in the same period (Pons-Branchu, 2015). The differences between the two profiles can be explained by mixing with other sources, but also by loss or partitioning effects during transport of the PAHs from the surface to the USCD.

4.2. PAH transport processes

4.2.1. The role of OM in PAH transport

PAHs are generally poorly soluble compounds which tend to be linked to OM content of natural waters and soils (Santschi et al., 1997). Humic-like (HL) molecules are the major components of the soil OM and of the dissolved OM (DOM) in natural waters. Their high molecular weight and aromaticity lead to the sorption of hydrophobic molecules such as PAHs (e.g. Jones et al., 1989).

A strong correlation was thus expected between PAH and OC concentrations in USCD. However, as observed in Desaules et al. (2008), no linear correlation was found between PAHs and OC (Fig.6.a, R^2 0.04, n=16). Depending on the historical period considered, this could be explained either by an excess of OM quantity relative to PAH concentration, or by a higher rate of PAH sorption on OM. The context of urbanisation and soil sealing (Fig.4) supports the idea of a low availability of OM and therefore an increase in PAH sorption on small quantities of OM during periods of higher PAH emissions. In addition, as most of the high PAH concentration samples contain mainly LMW PAHs, with elevated aqueous solubility and low Kow value, transport of PAHs from soil surface to USCD could have been in the dissolved phase.

Furthermore, variations in DOM quality occurred over time (Fig. 3). The blue-shift observed in the 1760s is associated with lower molecular weight or less aromatic organic molecules. This change could be linked to a change in agricultural practices at this period. At the beginning of the 18th century, waste from Paris was used as fertilizer in the surrounding area (Pons-Branchu et al., 2015), and it is possible that these practices ended in the vicinity of the site after the second half of the 18th century. However, no change in nitrogen was observed during this period. In contrast, a greater contribution of more aromatic molecules (red-shift) was observed during the urbanisation phase. Moreover, contrary to Quiers et al. (2015), it was not possible to model all SPF data with LPF (S1) and OC measurements to obtain quantitative variations of OC at high resolution. This supports the hypothesis of strong quality changes in organic molecules over

time, probably linked to changes in surface soils. For example, the addition of gypsum when land was levelled on the surface for the construction of buildings may have led to a change in ionic strength, which may have modified the adsorption conditions. In addition, these elements raise many questions about the origin and nature of OM, because the notion of soil in an urban context is very different from that of soil in a natural environment, as urban soils can have similar characteristics to natural soils or differ fundamentally from them (Lehmann and Stahr, 2007).

4.2.2. Transport by the particulate detrital phase.

Thorium tends to adsorb strongly to clay and oxyhydroxide phases (Langmuir and Herman, 1980) and can bound with detrital particles (Ayalon et al., 1999, Meyer et al., 2012). It also tends to complex and precipitate in the presence of carbonates (LaFamme and Murray, 1987). Thorium can then be considered as a tracer of the particulate detrital phase in BEL2. The correlation (R^2=0.6, n=14) between OC and thorium content of the USCD (Fig.6.b) indicates a covariation between OM and detrital particles fluxes. The relationship between the sum of PAHs and thorium (Fig.6.c) seems to correlate with part of the samples including three of the increases in PAHs (R^2=0.82, n=9). In addition, the samples with a correlation between thorium and PAH concentrations include those corresponding to the urbanisation period (points 10, 11, 12, 13). This suggests that during this period PAH were mainly transported by detrital particles from top soils to the USCD. The sample 9, belonging to the end of urbanisation, corresponds to a clayey lamina, which explains the enrichment in thorium.

5. Conclusions

The experimental development of a protocol for PAH extraction from USCDs has highlighted the presence of PAHs in sub-surface water in urban environments for 300 years. The evolution of PAHs shows two major events caused by intensive urbanisation. First, the decline in the FLA/PYR ratio in the

1850s seems to highlight the massive urbanisation phase that Belleville underwent between 1825 and 1900 CE, and second, the increase in HMW PAHs over the last 50 years seems to be linked to a change in source explained mainly by urban street dust. These observations bear direct witness to the negative impact of urbanisation on the quality of the seepage water from the Belleville aqueduct, which was used massively for human consumption until the 19th century. The study also highlighted changes in the quality of the OM over time, linked to changes in the surface soils. This work therefore extends our knowledge of the long-term impact of human activity in urban areas on the transfer of pollutants into sub-surface waters. In addition, USCDs once again appear to have good potential as recorders of water quality and human practices. However, the conditions in which they are formed, and the processes involved in transporting contaminants such as PAHs are important factors that should not be overlooked for interpretation purposes.

Acknowledgements

The "Association des Sources du Nord" (Gérard Duserre, Jean-Luc Largier, Jacques Paulic) and the Mairie de Paris (Bureau des Edifices Culturels et Historiques — Direction des Affaires Culturelles) are thanked for giving access to the Belleville aqueduct and historical information. TC_TN analyses were performed using the geochemistry-mineralogy platform of ISTerre (OSUG-France), and D. Tisserand is acknowledged for her help in acquiring the data. N. Cottin (EDYTEM/USMB) is also thanked for her advice on the PAH analysis. This work was supported by the "HUNIWERS" project from the ANR (grant number 18-CE22-0009).

References

Argiriadis, E., Denniston, R.F., Barbante, C., 2019. Improved Polycyclic Aromatic Hydrocarbon

and *n* -Alkane Determination in Speleothems through Cleanroom Sample Processing. Anal. Chem. 91, 7007–7011. https://doi.org/10.1021/acs.analchem.9b00767

Arias, A.H., Vazquez-Botello, A., Tombesi, N., Ponce-Vélez, G., Freije, H., Marcovecchio, J., 2010. Presence, distribution, and origins of polycyclic aromatic hydrocarbons (PAHs) in sediments from Bahía Blanca estuary, Argentina. Environ Monit Assess 160, 301–314. https://doi.org/10.1007/s10661-008-0696-5

Baek, S.O., Field, R.A., Goldstone, M.E., Kirk, P.W., Lester, J.N., Perry, R., 1991. A review of atmospheric polycyclic aromatic hydrocarbons: Sources, fate and behavior. Water Air Soil Pollut 60, 279–300. https://doi.org/10.1007/BF00282628

Bates, B., Kundzewicz, Z.W., Wu, S., Palutikof, J. (Eds.), 2008. Climate change and water, IPCC Secretariat. ed, Technical Paper of the Intergovernmental Panel on Climate Change. Geneva.

Birdwell, J.E., Engel, A.S., 2010. Characterization of dissolved organic matter in cave and spring waters using UV–Vis absorbance and fluorescence spectroscopy. Organic Geochemistry 41, 270–280. https://doi.org/10.1016/j.orggeochem.2009.11.002

Box, G.E.P., Muller, M.E., 1958. A Note on the Generation of Random Normal Deviates. Ann. Math. Statist. 29, 610–611. https://doi.org/10.1214/aoms/1177706645

Brandt, H.C.A., De Groot, P.C., 2001. Aqueous leaching of polycyclic aromatic hydrocarbons from bitumen and asphalt. Water Research 35, 4200–4207. https://doi.org/10.1016/S0043-1354(01)00216-0

Brown, J.N., Peake, B.M., 2006. Sources of heavy metals and polycyclic aromatic hydrocarbons in urban stormwater runoff. Science of the Total Environment.

Burek, P., Satoh, Y., Fisher, G., Kahil, M.T., Scherzer, A., 2016. Water futures and solution-fast track initiative. International Institute for Applied Systems Analysis.

Clément, A., Thomas, G., 2016. Atlas du Paris souterrain: la doublure sombre de la Ville lumière., Parigramme. ed. Paris.

Coble, P.G., 1996. Characterization of marine and terrestrial DOM in seawater using excitation-emission matrix spectroscopy. Marine Chemistry 51, 325–346. https://doi.org/10.1016/0304-4203(95)00062-3

De La Torre-Roche, R.J., Lee, W.-Y., Campos-Díaz, S.I., 2009. Soil-borne polycyclic aromatic hydrocarbons in El Paso, Texas: Analysis of a potential problem in the United States/Mexico border region. Journal of Hazardous Materials 163, 946–958. https://doi.org/10.1016/j.jhazmat.2008.07.089

Desaules, A., Ammann, S., Blum, F., Brändli, R.C., Bucheli, T.D., Keller, A., 2008. PAH and PCB in soils of Switzerland—status and critical review. J. Environ. Monit. 10, 1265. https://doi.org/10.1039/b807206j

Du, J., Jing, C., 2018. Anthropogenic PAHs in lake sediments: a literature review (2002–2018). Environ. Sci.: Processes Impacts 20, 1649–1666. https://doi.org/10.1039/C8EM00195B

Fernandez, M., 2018. La strate du sol d'une mégapole : observations localisées sur l'Anthropocène: Les couches issues des périodes préindustrielle et industrielle à Paris. geocarrefour 92. https://doi.org/10.4000/geocarrefour.12016

Freeman, D.J., Cattell, F.C.R., 1990. Woodburning as a source of atmospheric polycyclic aromatic hydrocarbons. Environ. Sci. Technol. 24, 1581–1585. https://doi.org/10.1021/es00080a019

Gonzalez, A., Moilleron, R., Chebbo, G., Thévenot, D.R., 2000. Determination of Polycyclic Aromatic Hydrocarbons in Urban Runoff Samples from the "Le Marais" Experimental Catchment in Paris Centre. Polycyclic Aromatic Compounds 20, 1–19. https://doi.org/10.1080/10406630008034772

Grimalt, J.O., Van Drooge, B.L., Ribes, A., Fernández, P., Appleby, P., 2004. Polycyclic aromatic hydrocarbon composition in soils and sediments of high altitude lakes. Environmental Pollution 131, 13–24. https://doi.org/10.1016/j.envpol.2004.02.024

Guo, Z., Lin, T., Zhang, G., Zheng, M., Zhang, Z., Hao, Y., Fang, M., 2007. The sedimentary fluxes of polycyclic aromatic hydrocarbons in the Yangtze River Estuary coastal sea for the past century. Science of The Total Environment 386, 33–41. https://doi.org/10.1016/j.scitotenv.2007.07.019

Hangebrauck, R.P., Lehmden, D.J.V., Meeker, J.E., 1967. Sources of Polynuclear Hydrocarbons in the Atmosphere, Environmental health series. U.S. Department of Health, Education, and Welfare [National Center for Air Pollution Control].

Hartland, A., Fairchild, I.J., Müller, W., Dominguez-Villar, D., 2014. Preservation of NOM-metal complexes in a modern hyperalkaline stalagmite: Implications for speleothem trace element geochemistry. Geochimica et Cosmochimica Acta 128, 29–43. https://doi.org/10.1016/j.gca.2013.12.005

Hoffman, E.J., Mills, G.L., Latimer, J.S., Quinn, J.G., 1984. Urban runoff as a source of polycyclic aromatic hydrocarbons to coastal waters. Environ. Sci. Technol. 18, 580–587. https://doi.org/10.1021/es00126a003

Huard, M., 2019. Atlas historique de Paris, Persée. ed.

Hudson, N., Baker, A., Reynolds, D., 2007. Fluorescence analysis of dissolved organic matter in natural, waste and polluted waters—a review. River Res. Applic. 23, 631–649. https://doi.org/10.1002/rra.1005

Jiménez Cisneros, B.E., Oki, T., Arnel, N.W., Benito, G., Cogley, J.G., Döll, P., Jiang, T., Mwakalila, S.S., 2014. Freshwater Resources, in: Climate Change 2014: Impacts, Adaptation, and Vulnerability. Part A: Global and Sectoral Aspects. Contribution of

Working Group II to the Fifth Assessment Report of the Intergovernmental Panel on Climate Change. Cambridge University Press, Cambridge, United Kingdom and New York, NY, USA, pp. 229–269.

Jones, K.C., Stratford, J.A., Tidridge, P., Waterhouse, K.S., Johnston, A.E., 1989. Polynuclear aromatic hydrocarbons in an agricultural soil: Long-term changes in profile distribution. Environmental Pollution 56, 337–351. https://doi.org/10.1016/0269-7491(89)90079-1

Kakareka, S.V., Kukharchyk, T.I., 2003. PAH emission from the open burning of agricultural debris. Science of The Total Environment 308, 257–261. https://doi.org/10.1016/S0048-9697(02)00650-2

Katsoyiannis, A., Breivik, K., 2014. Model-based evaluation of the use of polycyclic aromatic hydrocarbons molecular diagnostic ratios as a source identification tool. Environmental Pollution 184, 488–494. https://doi.org/10.1016/j.envpol.2013.09.028

Katsoyiannis, A., Sweetman, A.J., Jones, K.C., 2011. PAH Molecular Diagnostic Ratios Applied to Atmospheric Sources: A Critical Evaluation Using Two Decades of Source Inventory and Air Concentration Data from the UK. Environ. Sci. Technol. 45, 8897–8906. https://doi.org/10.1021/es202277u

Lehmann, A., Stahr, K., 2007. Nature and significance of anthropogenic urban soils. J Soils Sediments 7, 247–260. https://doi.org/10.1065/jss2007.06.235

Ligtvoet, W., Hilderink, H., Bouwman, A., Puijenbroek, P., Lucas, P., Witmer, M., 2014. Towards a world of cities in 2050 - An outlook on water- related challenges (Background report to the UN-Habitat Global Report). PBL Netherlands Environmental Assessment Agency.

Liu, S., Xia, X., Yang, L., Shen, M., Liu, R., 2010. Polycyclic aromatic hydrocarbons in urban soils of different land uses in Beijing, China: Distribution, sources and their correlation

with the city's urbanization history. Journal of Hazardous Materials 177, 1085–1092. https://doi.org/10.1016/j.jhazmat.2010.01.032

McVeety, B.D., Hites, R.A., 1988. Atmospheric deposition of polycyclic aromatic hydrocarbons to water surfaces: A mass balance approach. Atmospheric Environment (1967) 22, 511–536. https://doi.org/10.1016/0004-6981(88)90196-5

Méot, T., 2009. L'industrie automobile en France depuis 1950 : des mutations à la chaîne, L'économie française - Comptes et dossiers. Inee.

Moya, A., Giraud, F., Molinier, V., Perrette, Y., Charlet, L., Van Driessche, A., Fernandez-Martinez, A., 2023. Exploring carbonate rock wettability across scales: Role of (bio)minerals. Journal of Colloid and Interface Science 642, 747–756. https://doi.org/10.1016/j.jcis.2023.03.197

Müller, A., Österlund, H., Marsalek, J., Viklander, M., 2020. The pollution conveyed by urban runoff: A review of sources. Science of The Total Environment 709, 136125. https://doi.org/10.1016/j.scitotenv.2019.136125

Ngabe, B., 2000. Polycyclic aromatic hydrocarbons in storm runoff from urban and coastal South Carolina. The Science of The Total Environment 255, 1–9. https://doi.org/10.1016/S0048-9697(00)00422-8

Pereira, W.E., Hostettler, F.D., Luoma, S.N., Van Geen, A., Fuller, C.C., Anima, R.J., 1999. Sedimentary record of anthropogenic and biogenic polycyclic aromatic hydrocarbons in San Francisco Bay, California. Marine Chemistry 64, 99–113. https://doi.org/10.1016/S0304-4203(98)00087-5

Perrette, Y., Poulenard, J., Durand, A., Quiers, M., Malet, E., Fanget, B., Naffrechoux, E., 2013. Atmospheric sources and soil filtering of PAH content in karst seepage waters. Organic Geochemistry 65, 37–45. https://doi.org/10.1016/j.orggeochem.2013.10.005

Perrette, Y., Poulenard, J., Saber, A.-I., Fanget, B., Guittonneau, S., Ghaleb, B., Garaudee, S., 2008. Polycyclic Aromatic Hydrocarbons in stalagmites: Occurrence and use for analyzing past environments. Chemical Geology 251, 67–76. https://doi.org/10.1016/j.chemgeo.2008.02.013

Pons-Branchu, E., Ayrault, S., Roy-Barman, M., Bordier, L., Borst, W., Branchu, P., Douville, E., Dumont, E., 2015. Three centuries of heavy metal pollution in Paris (France) recorded by urban speleothems. Science of The Total Environment 518–519, 86–96. https://doi.org/10.1016/j.scitotenv.2015.02.071

Pons-Branchu, E., Douville, E., Roy-Barman, M., Dumont, E., Branchu, P., Thil, F., Frank, N., Bordier, L., Borst, W., 2014. A geochemical perspective on Parisian urban history based on U–Th dating, laminae counting and yttrium and REE concentrations of recent carbonates in underground aqueducts. Quaternary Geochronology 24, 44–53. https://doi.org/10.1016/j.quageo.2014.08.001

Pons-Branchu, E., Roy-Barman, M., Joan-Soro, L., Guillerme, A., Branchu, P., Fernandez, M., Dumont, E., Douville, E., Michelot, J., Phillips, A., 2017. Urbanization impact on sulfur content of groundwater revealed by the study of urban speleothem-like deposits: Case study in Paris, France. Science of The Total Environment 579, 124–132. https://doi.org/10.1016/j.scitotenv.2016.10.234

Quiers, M., Perrette, Y., Chalmin, E., Fanget, B., Poulenard, J., 2015. Geochemical mapping of organic carbon in stalagmites using liquid-phase and solid-phase fluorescence. Chemical Geology 411, 240–247. https://doi.org/10.1016/j.chemgeo.2015.07.012

Ravindra, K., Sokhi, R., Vangrieken, R., 2008. Atmospheric polycyclic aromatic hydrocarbons: Source attribution, emission factors and regulation. Atmospheric Environment 42, 2895–2921. https://doi.org/10.1016/j.atmosenv.2007.12.010

Rocher, V., Azimi, S., Moilleron, R., Chebbo, G., 2004. Hydrocarbons and heavy metals in the different sewer deposits in the 'Le Marais' catchment (Paris, France): stocks, distributions and origins. Science of The Total Environment 323, 107–122. https://doi.org/10.1016/j.scitotenv.2003.10.010

Santschi, P.H., Lenhart, J.J., Honeyman, B.D., 1997. Heterogeneous processes affecting trace contaminant distribution in estuaries: The role of natural organic matter. Marine Chemistry 58, 99–125. https://doi.org/10.1016/S0304-4203(97)00029-7

Shen, H., Tao, S., Wang, R., Wang, B., Shen, G., Li, W., Su, S., Huang, Y., Wang, X., Liu, W., 2011. Global time trends in PAH emissions from motor vehicles. Atmos Environ 45, 2067–2073. https://doi.org/10.1016/j.atmosenv.2011.01.054

Soclo, H.H., Garrigues, P., Ewald, M., 2000. Origin of Polycyclic Aromatic Hydrocarbons (PAHs) in Coastal Marine Sediments: Case Studies in Cotonou (Benin) and Aquitaine (France) Areas. Marine Pollution Bulletin 40, 387–396. https://doi.org/10.1016/S0025-326X(99)00200-3

Staninska, J., Szczepaniak, Z., Cyplik, P., Piotrowska-Cyplik, A., 2015. The effect of organic and clay fraction on polycyclic aromatic hydrocarbons mobility in soil model systems. Journal of Research and Applications in Agricultural Engineering 60, 98–101.

Stout, S.A., Uhler, A.D., Emsbo-Mattingly, S.D., 2004. Comparative Evaluation of Background Anthropogenic Hydrocarbons in Surficial Sediments from Nine Urban Waterways. Environ. Sci. Technol. 38, 2987–2994. https://doi.org/10.1021/es040327q

Suman, S., Sinha, A., Tarafdar, A., 2016. Polycyclic aromatic hydrocarbons (PAHs) concentration levels, pattern, source identification and soil toxicity assessment in urban traffic soil of Dhanbad, India. Science of The Total Environment 545–546, 353–360. https://doi.org/10.1016/j.scitotenv.2015.12.061

Takada, H., Onda, T., Harada, M., Ogura, N., 1991. Distribution and sources of polycyclic aromatic hydrocarbons (PAHs) in street dust from the Tokyo Metropolitan area. Science of The Total Environment 107, 45–69. https://doi.org/10.1016/0048-9697(91)90249-E

Tissier, G., Perrette, Y., Dzikowski, M., Poulenard, J., Hobléa, F., Malet, E., Fanget, B., 2013. Seasonal changes of organic matter quality and quantity at the outlet of a forested karst system (La Roche Saint Alban, French Alps). Journal of Hydrology.

Tobiszewski, M., Namieśnik, J., 2012. PAH diagnostic ratios for the identification of pollution emission sources. Environmental Pollution 162, 110–119. https://doi.org/10.1016/j.envpol.2011.10.025

Tuominen, Jari., Salomaa, Sisko., Pyysalo, Heikki., Skytta, Eija., Tikkanen, Leena., Nurmela, Tuomo., Sorsa, Marja., Pohjola, Veijo., Sauri, Marketta., Himberg, Kimmo., 1988. Polynuclear aromatic compounds and genotoxicity in particulate and vapor phases of ambient air: effect of traffic, season and meteorological conditions. Environ. Sci. Technol. 22, 1228–1234. https://doi.org/10.1021/es00175a017

United Nations, Department of Economic and Social Affairs, 2022. The Sustainable Development Goals Report 2022. UN.

Wynn, P.M., Brocks, J.J., 2014. A framework for the extraction and interpretation of organic molecules in speleothem carbonate: Extracting and interpreting organic molecules in speleothems. Rapid Commun. Mass Spectrom. 28, 845–854. https://doi.org/10.1002/rcm.6843

Yu, B., Xie, X., Ma, L.Q., Kan, H., Zhou, Q., 2014. Source, distribution, and health risk assessment of polycyclic aromatic hydrocarbons in urban street dust from Tianjin, China. Environ Sci Pollut Res 21, 2817–2825. https://doi.org/10.1007/s11356-013-2190-z

Zhang, W., Zhang, S., Wan, C., Yue, D., Ye, Y., Wang, X., 2008. Source diagnostics of

polycyclic aromatic hydrocarbons in urban road runoff, dust, rain and canopy throughfall. Environmental Pollution 153, 594–601. https://doi.org/10.1016/j.envpol.2007.09.004

Zhang, X.L., Tao, S., Liu, W.X., Yang, Y., Zuo, Q., Liu, S.Z., 2005. Source Diagnostics of Polycyclic Aromatic Hydrocarbons Based on Species Ratios: A Multimedia Approach. Environ. Sci. Technol. 39, 9109–9114. https://doi.org/10.1021/es0513741

Fig. 1. Site presentation a) Location of the Aqueduct of Belleville, sampled site and schematic geological cross-section (modified from Pons-Branchu et al., 2015); b) Sampled section view; c) On the left, PAH sampling plan on a section of BEL2 USCD and, on the right, reference axis with the location of all the samplings (Organic carbon (OC), total nitrogen (TN), liquid phase fluorescence (LPF), trace elements (TE)).

Fig. 2. PAH distributions in BEL2. On the left part, in white the sum of PAHs in $ng.g^{-1}$ with the relative error together with a stacked histogram (in %) of LMW PAHs (light blue) and HMW PAHs (dark blue). On the right part, PAH distributions (normalized concentrations in %) of each sample with N: Naphthalene, Ace: Acenaphthene, Flu: Fluorene, Phe: Phenanthrene, Ant: Anthracene, Fla: Fluoranthene, Pyr: Pyrene, BaA: Benzo[a]Anthracene, Chr: Chrysene, BbF: Benzo[b]Fluorene, BkF: Benzo[k]Fluoranthene, BaP: Benzo[a]Pyrene, BghiP: Benzo[ghi]Perylene, DbahA: Dibenzo[ah]Anthracene, IP: Indeno[1,2,3-cd]Pyrene.

Fig. 3. Representation of the four log-normal functions fitted to a SPF measured mean spectrum (black curve). Function 1 is centered at 350 nm ± 20 nm, function 2 at 420 ± 20 nm, function 3 at 500 ± 20 nm. Function 4 corresponds to NIR diode reflection. The resulting simulated spectrum is represented in dashed blue. On the right, the intensity ratio map between functions 2 and 3; the dark areas correspond to organic carbon and LPF samples.

Fig.4. PAHs and chronological context. The four Belleville urbanisation maps are extracted and modified from Huard (2019). The demography (Pop.) is express in inhabitants and result in a combination of the demography in Belleville before 1860 from EHESS (http://cassini.ehess.fr/fr/html/), and the demography of the 19th and 20th districts of Paris recorded by Insee after 1860 (https://www.insee.fr/fr/statistiques/3698339). The sources identified by the FLA/(FLA+PYR) ratio are represented by icons on the left: values < 0.4 correspond to petrogenic sources, the values > 0.5 to grass, wood, or coal combustion, and values between 0.4 and 0.5 to fossil fuel combustion.

Fig.5. a. Relationship between LMW PAHs in $ng.g^{-1}$ and the sum of PAHs. **b.** On the left, profiles of the relative concentrations in urban dust from SRM 1649a (certificate values) and in BEL2_1 (1995-2011 CE) measured sample. On the right, plot of BEL2_1 measured concentrations (% of the total PAHs) vs Urban dust concentrations (% of the total PAHs).

Fig. 6. a. The relationship between the sum of PAHs in $ng.g^{-1}$ and OC in $mg.g^{-1}$. Orange dots correspond to PAH increases. **b.** The relationship between OC in $mg.g^{-1}$and Th in $\mu g.g^{-1}$ (from Pons-Branchu et al. (2015)), points 4, 6, and 17 have no associated value in Th and do not appear on the graph. **c.** The relationship between the sum of PAHs in $ng.g^{-1}$ and Th in $\mu g.g^{-1}$.

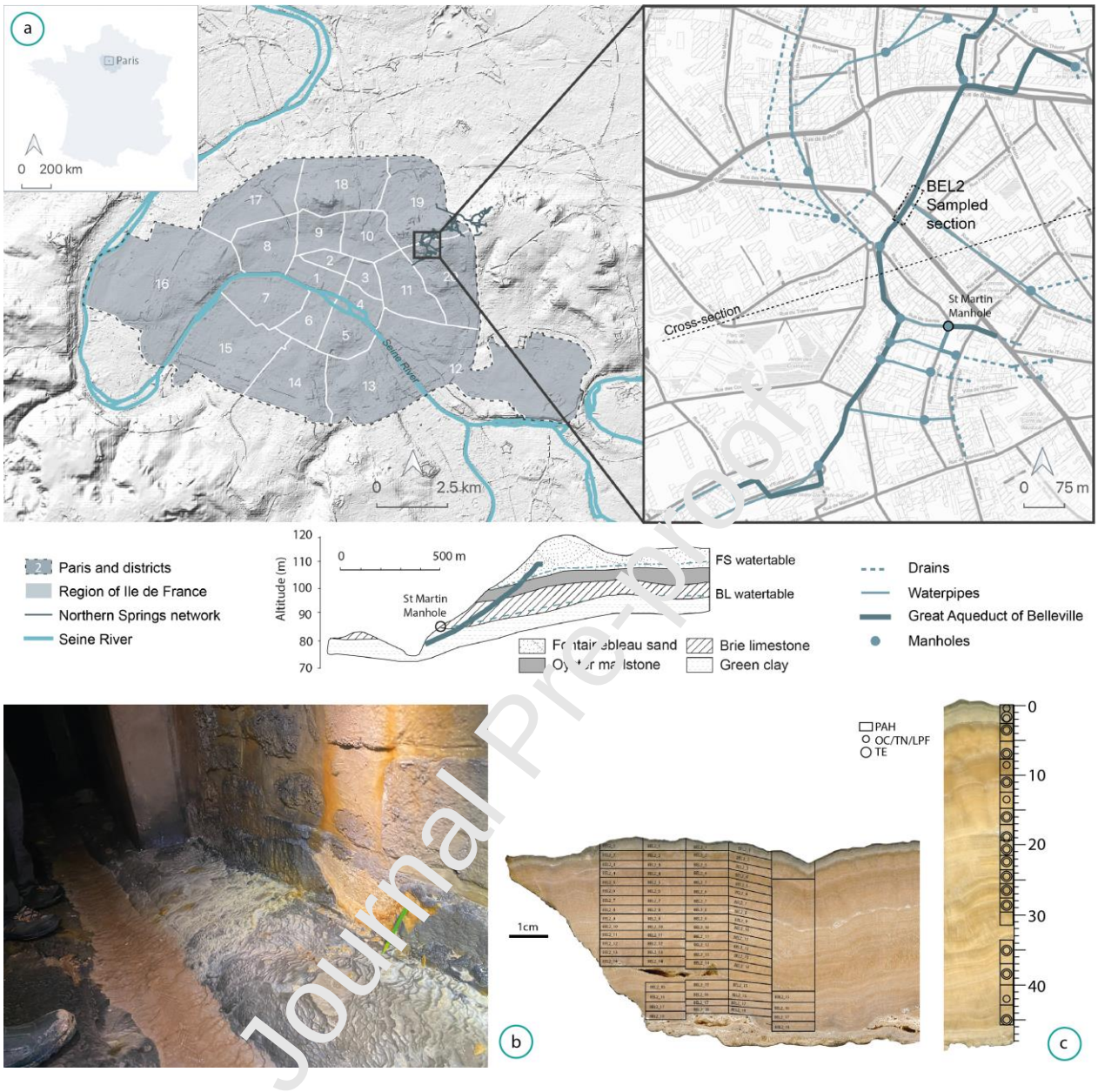

Fig. 1

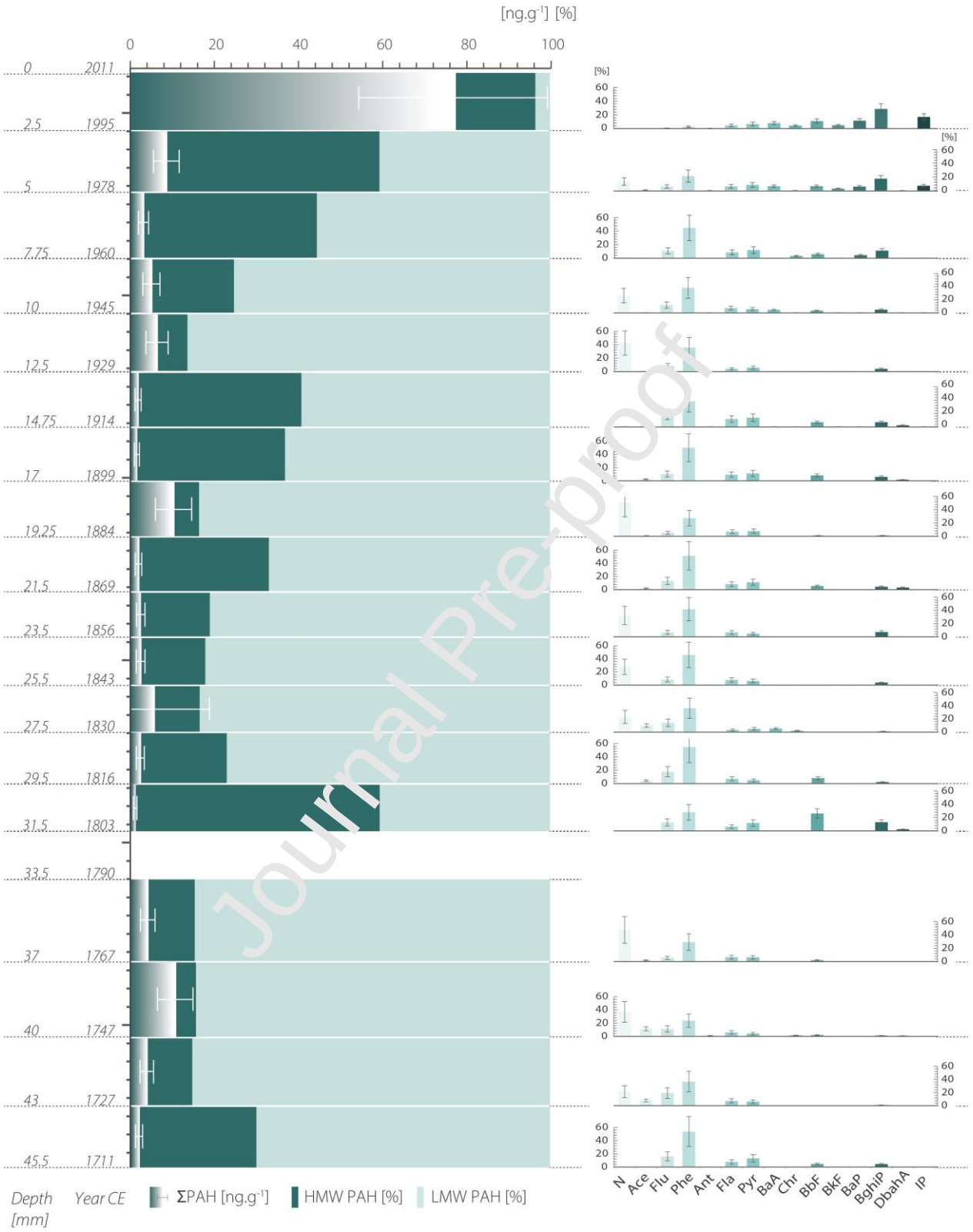
[ng.g-1] [%]
0
20
40
60
80
100
Depth [mm]
Year CE
0 2011
2.5 1995
5 1978
7.75 1960
10 1945
12.5 1929
14.75 1914
17 1899
19.25 1884
21.5 1869
23.5 1856
25.5 1843
27.5 1830
29.5 1816
31.5 1803
33.5 1790
37 1767
40 1747
43 1727
45.5 1711
ΣPAH [ng.g-1]
HMW PAH [%]
LMW PAH [%]
[%]
60
40
20
0
N
Ace
Flu
Phe
Ant
Fla
Pyr
BaA
Chr
BbF
BkF
BaP
BghiP
DbahA
IP

Fig. 2

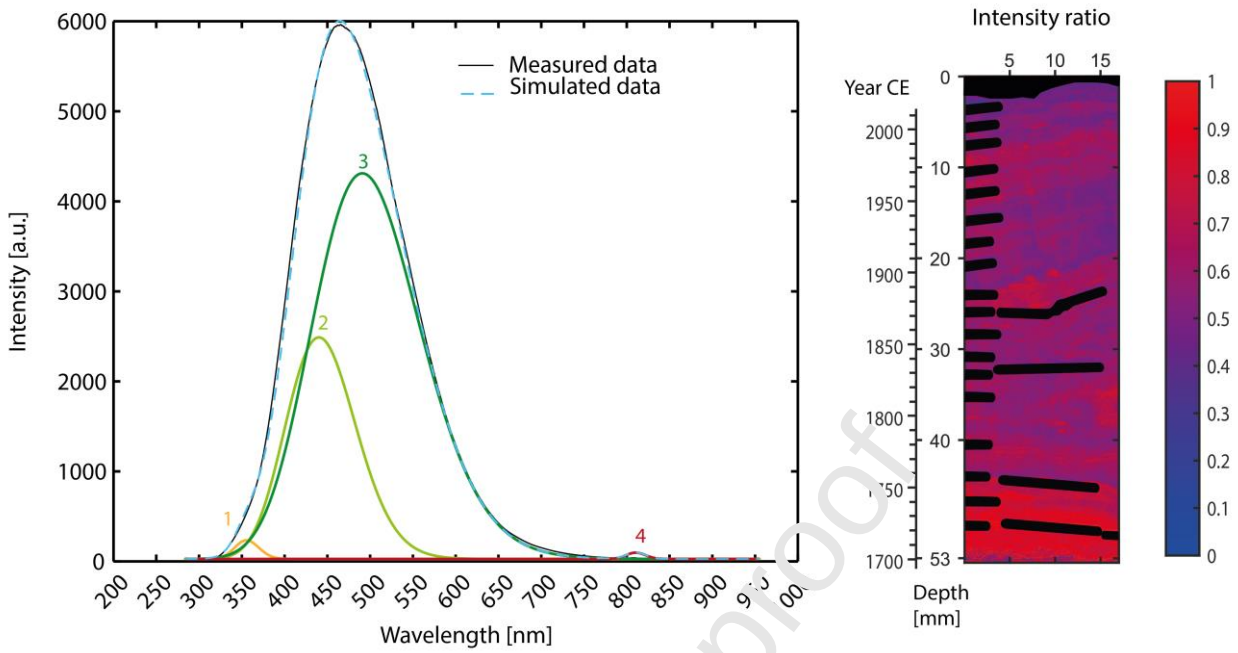

Fig. 3

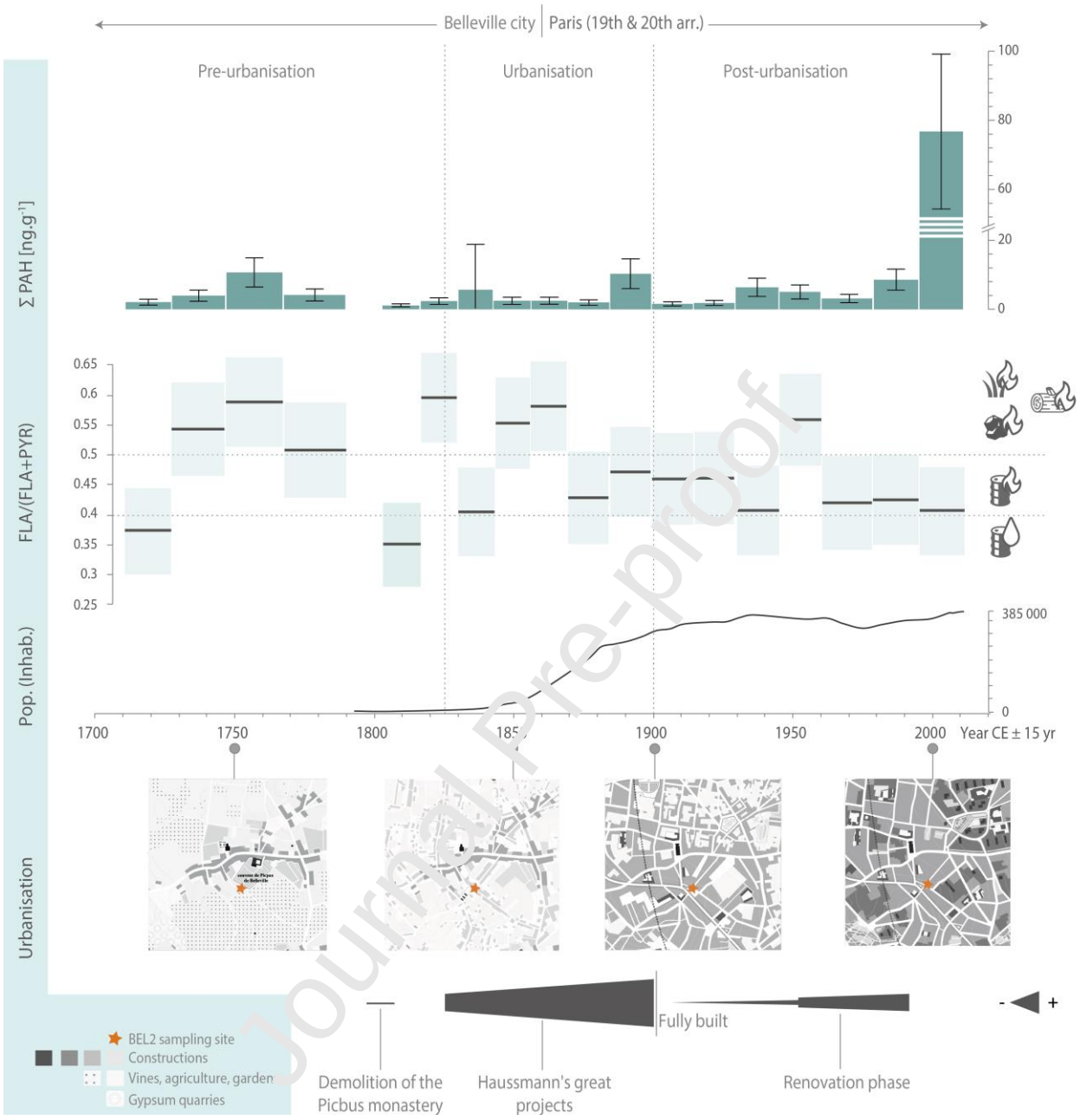

Fig. 4

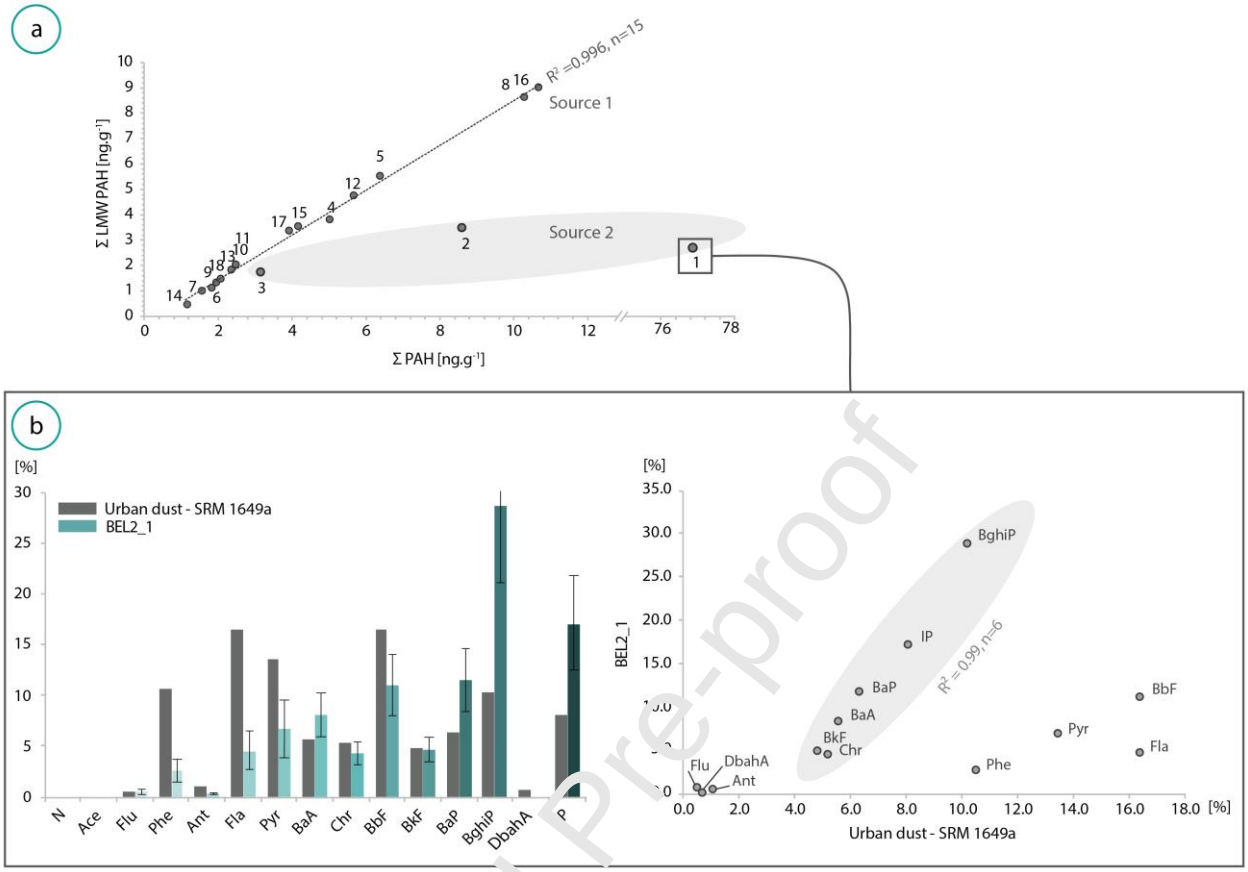

Fig. 5

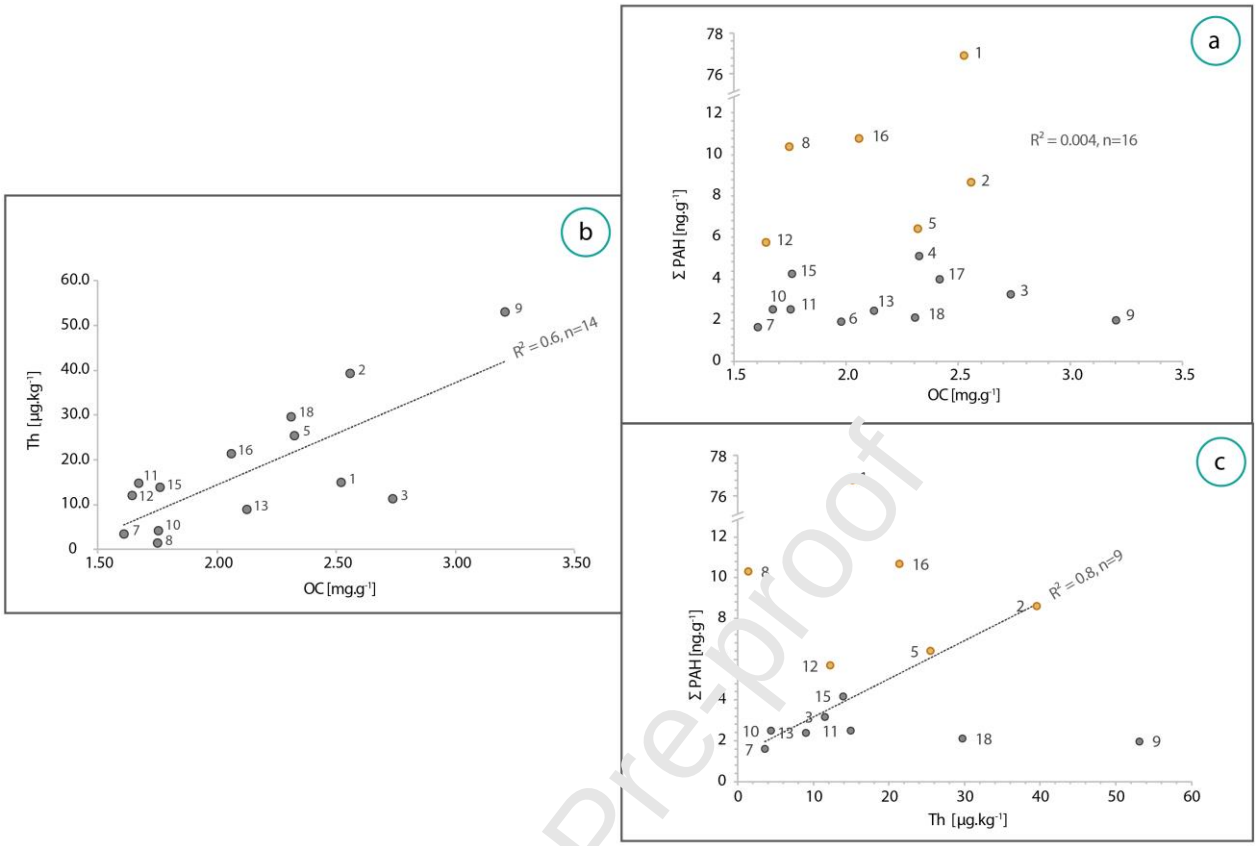

Fig. 6

Top Age	Bottom Age	Relative top depth	Relative bottom depth	Sample	N	Ace	Flu	Phe	Ant	Fla	Pyr	BaA	Chr	BbF	BkF	BaP	BghiP	DbahA	IP	ΣPAHs	ΣLMW PAHs	ΣHMW PAHs
2011	1995	0	2.5	BEL2-1	LOB	LOD	0.4	2.0	0.2	3.5	5.1	6.2	3.3	8.4	3.6	8.8	22.0	NA	13.1	76.8	2.7	74.1
1995	1978	2.5	5	BEL2-2	1.1	***0.06***	0.5	1.8	LOD	0.5	0.7	0.5	LOD	0.5	0.2	0.5	1.5	NA	***0.6***	8.6	3.5	5.1
1978	1960	5	7.75	BEL2-3	LOB	LOD	0.3	1.4	LOD	0.3	0.4	LOD	***0.1***	0.2	LOD	***0.1***	0.4	LOD	LOD	3.2	1.8	1.4
1960	1945	7.75	10	BEL2-4	1.3	LOD	0.6	1.9	LOD	0.4	0.3	***0.2***	LOD	0.2	LOD	LOD	0.2	LOD	LOD	5.0	3.8	1.2
1945	1929	10	12.5	BEL2-5	2.7	LOD	0.5	2.3	LOD	0.3	0.4	LOD	LOD	LOD	LOD	LOD	0.3	NA	LOD	6.4	5.5	0.9
1929	1914	12.5	14.75	BEL2-6	LOB	***0.05***	0.3	0.7	LOD	0.2	0.3	LOD	LOD	0.1	LOD	LOD	0.1	***0.04***	LOD	1.8	1.1	0.8
1914	1899	14.75	17	BEL2-7	LOB	***0.04***	***0.2***	0.8	LOD	0.2	0.2	LOD	LOD	0.1	LOD	LOD	0.1	***0.03***	LOD	1.6	1.0	0.6
1899	1884	17	19.25	BEL2-8	5.2	***0.07***	0.5	2.8	LOD	0.7	0.8	LOD	LOD	***0.09***	LOD	LOD	0.1	LOD	LOD	10.3	8.6	1.7
1884	1869	19.25	21.5	BEL2-9	LOB	***0.04***	0.3	1.0	LOD	0.2	0.2	LOD	LOD	0.1	LOD	LOD	0.1	0.06	LOD	2.0	1.3	0.7
1869	1856	21.5	23.5	BEL2-10	0.8	LOD	***0.2***	1.0	LOD	0.2	0.1	LOD	LOD	LOD	LOD	LOD	0.2	LOD	LOD	2.5	2.0	0.5
1856	1843	23.5	25.5	BEL2-11	0.7	LOD	***0.2***	1.1	LOD	0.2	0.2	LOD	LOD	LOD	LOD	LOD	0.09	LOD	LOD	2.5	2.0	0.4
1843	1830	25.5	27.5	BEL2-12	1.3	0.6	0.8	2.1	LOD	0.2	0.3	***0.3***	***0.1***	LOD	LOD	LOD	***0.05***	LOD	LOD	5.7	4.7	0.9
1830	1816	27.5	29.5	BEL2-13	LOB	0.1	0.4	1.3	LOD	0.2	0.1	LOD	LOD	0.2	LOD	LOD	***0.05***	LOD	LOD	2.4	1.8	0.5
1816	1803	29.5	31.5	BEL2-14	LOB	LOD	***0.2***	0.3	LOD	0.1	0.1	LOD	LOD	0.2	LOD	LOD	0.2	***0.03***	LOD	1.2	0.5	0.7
1790	1767	33.5	37	BEL2-15	2.0	***0.09***	0.2	1.2	LOD	0.3	0.3	LOD	LOD	***0.09***	LOD	LOD	LOD	LOD	LOD	4.2	3.5	0.6
1767	1747	37	40	BEL2-16	3.9	1.2	1.2	2.5	***0.1***	0.1	0.2	LOD	***0.2***	0.2	LOD	LOD	0.1	0.08	LOD	10.7	9.0	1.7
1747	1727	40	43	BEL2-17	0.8	0.3	0.8	1.4	LOD	0.3	0.3	LOD	LOD	LOD	LOD	LOD	***0.04***	LOD	LOD	3.9	3.4	0.6
1727	1711	43	45.5	BEL2-18	LOB	LOD	0.3	1.1	LOD	0.2	0.3	LOD	LOD	***0.1***	LOD	LOD	0.09	NA	LOD	2.1	1.5	0.6
1914	1899	14.75	17	BEL2_7R	0.7	0.5	21.4	1.8	***0.10***	0.4	0.4	1.3	0.2	0.3	LOD	LOD	***0.05***	LOD	LOB	27.1	24.5	2.6
1899	1884	17	19.25	BEL2_8R	2.9	***0.08***	0.7	1.8	LOD	0.5	0.3	LOD	***0.1***	LOD	LOD	LOD	***0.04***	LOD	LOB	6.5	5.5	1.0
1884	1869	19.25	21.5	BEL2_9R	LOB	LOD	LOB	LOB	LOD	LOB	LOB	LOB	LOD	***0.09***	LOB	LOB	LOB	***0.03***	LOB	0.1	0.0	0.1
1869	1856	21.5	23.5	BEL2_10R	LOB	LOB	LOB	LOB	LOD	0.2	LOB	LOB	LOB	LOD	LOB	LOD	0.07	LOD	LOB	0.3	0.0	0.3
1856	1843	23.5	25.5	BEL2_11R	LOB	***0.06***	LOB	LOB	LOD	0.2	0.6	LOB	LOD	LOD	LOD	LOD	LOB	LOD	LOB	0.9	0.06	0.8
1843	1830	25.5	27.5	BEL2_12R	3.0	***0.08***	1.0	2.6	***0.09***	0.8	0.8	LOD	LOB	LOD	LOD	LOD	LOB	LOD	LOB	8.4	6.8	1.6
1830	1816	27.5	29.5	BEL2_13R	0.8	LOB	LOB	LOB	LOD	0.2	0.2	LOB	LOD	LOD	LOB	LOD	LOB	***0.03***	LOD	1.2	0.8	0.4
1790	1767	33.5	37	BEL2_15R	1.8	0.2	LOB	2.6	LOD	1.1	0.4	LOD	0.2	***0.09***	LOD	LOD	LOB	LOD	LOB	6.3	4.6	1.7
1767	1747	37	40	BEL2_16R	3.1	0.8	LOB	0.8	LOD	0.2	0.2	LOD	LOB	1.3	LOB	NA	0.08	***0.03***	LOB	6.3	4.6	1.7
1747	1727	40	43	BEL2_17R	0.5	0.3	LOB	1.5	LOD	0.3	0.3	***0.2***	0.2	LOB	LOD	LOD	***0.04***	LOD	LOB	3.4	2.3	1.1

Table 1. PAH concentrations in BEL2 [ng.g^{-1}]. Naphthalene (N), Acenaphthene (Ace), Fluorene (Flu), Phenanthrene (Phe), Anthracene (ant), Fluoranthene (Fla), Pyrene (Pyr), Benzo[a]Anthracene (BaA), Chrysene (Chr), Benzo[b]Fluorene (BbF), Benzo[k]Fluoranthene (BkF), Benzo[a]Pyrene (BaP), Benzo[ghi]Perylene (BghiP), Dibenzo[ah]Anthracene (DbahA), Indeno[1,2,3-cd]Pyrene (IP). Concentrations in Italic Bold are below LOQ. Concentrations measured below blank (LOB) or LOD were assumed to be zero. The age is expressed in Year CE. The uncertainties are shown in Fig.2

Age	Relative Depth	Sampling Depth	Name	OC ($mg.g^{-1}$)	± ΔOC ($mg.g^{-1}$)	TN ($mg.g^{-1}$)	± ΔTN ($mg.g^{-1}$)
2008	0.5	0.5	BEL2-0	2.733	0.428	0.106	0.023
1999	1.75	2.5	BEL2-1	2.304	0.361	0.088	0.019
1988	3.5	4.5	BEL2-2	2.557	0.400	0.082	0.018
1965	7	7.5	BEL2-3	2.735	0.428	0.072	0.015
1955	8.5	9.75	BEL2-4	2.329	0.365	0.076	0.016
1938	11	12.75	BEL2-5	2.324	0.364	0.065	0.014
1922	13.5	15.25	BEL2-6	1.982	0.310	0.063	0.014
1906	16	17.5	BEL2-7	1.611	0.25[illegible]	0.048	0.010
1886	19	19.5	BEL2-8	1.750	0.27[illegible]	0.045	0.010
1876	20.5	21.5	BEL2_9	3.205	0.[illegible]02	0.056	0.012
1863	22.5	24	BEL2_10	1.755	0.2[illegible]5	0.046	0.010
1849	24.5	26.25	BEL2_11	1.672	[illegible]	0.042	0.009
1836	26.5	28	BEL2_12	1.643	0.257	0.064	0.014
1823	28.5	30.75	BEL2_13	2.12[illegible]	0.333	0.056	0.012
1780	35	35.5	BEL2_15	1.76[illegible]	0.276	0.061	0.013
1757	38.5	39	BEL2_16	[illegible].058	0.469	0.075	0.017
1734	42	42	BEL2_[illegible]7	[illegible].[illegible]17	0.378	0.064	0.014
1714	45	44.5	BEL2_18	2.312	0.362	0.078	0.017

Table 2. Organic carbon (OC), total nitrogen (TN) concentrations, expressed in $mg.g^{-1}$ with the associated error. Age is expressed in Year CE and depth in mm.

CRediT author statement

Julia Garagnon : Methodology, Investigation, Formal analysis, Validation, Writing - Original Draft, Visualization. **Yves Perrette** : Conceptualization, Software, Supervision, Writing - Review & Editing. **Emmanuel Naffrechoux** : Conceptualization, Validation, Supervision, Writing - Review & Editing. **Edwige Pons-Branchu** : Conceptualization, Resources, Supervision, Writing - Review & Editing, Project administration, Funding acquisition

Declaration of competing interest

The authors declare that they have no known competing financial interests or personal relationships that could have appeared to influence the work reported in this paper.

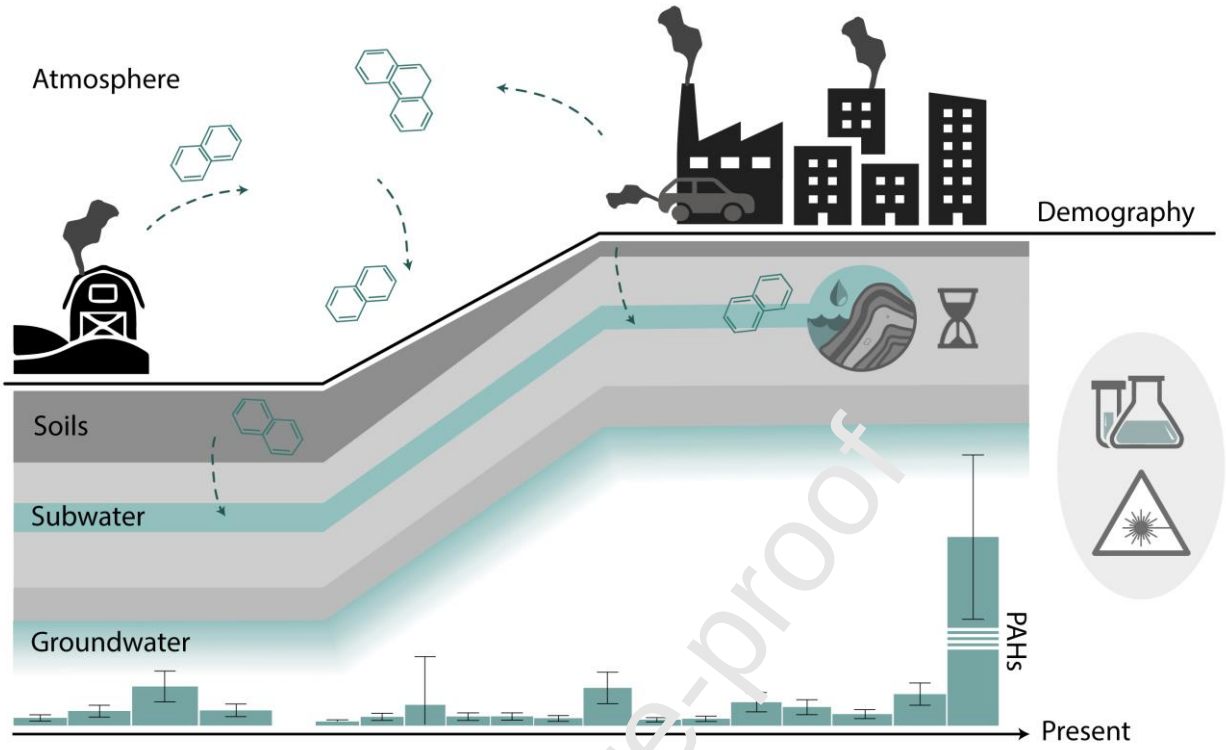

Graphical abstract

H I G H L I G H T S

- Speleothems are used to reconstruct surface water PAHs and organic matter content.
- PAHs have been present in urban surface water for 300 years.
- A major increase and a change of source occurred from the mid-20th century.
- Natural organic matter quality varies over time as a result of changes in land use.